Channel plasmon-polariton in a triangular groove on a metal surface

D. F. P. Pile, D. K. Gramotnev

Applied Optics Program, School of Physical and Chemical Sciences,

Queensland University of Technology, GPO Box 2434, Brisbane, QLD 4001, Australia.

ABSTRACT

One-dimensional localized plasmons (channel polaritons) guided by a triangular groove on a metal substrate are investigated numerically by means of finite-difference time-domain algorithm. Dispersion, existence conditions, and dissipation of these waves are analyzed. In particular, it is demonstrated that the localization of the predicted plasmons in acute grooves may be substantially stronger than what is allowed by the diffraction limit. As a result, the predicted waves may be of a significant importance for the development of new sub-wavelength waveguides and interconnectors for nano-optics and photonics.

OCIS codes: 130.0130, 130.2790, 240.0240, 260.3910, 350.3950.

One of the major directions of research in modern photonics and nano-optics is related to the theoretical and experimental investigation of new types of guided electromagnetic waves that can be used for the development of sub-wavelength waveguides and interconnectors beating the so-called diffraction limit of light [1-14]. This is because increasing speed and sensitivity of photonic devices heavily relies upon further miniaturization and integration of optical elements.

The main idea for the design of sub-wavelength interconnectors is based on the use of evanescent waves in media with negative real part of the dielectric permittivity, e.g., metals [1-3,6,8,9,12-14]. Within the last few years, a whole new area of nano-optics and photonics, related to surface plasmons in metallic nano-structures, has rapidly been developing [1-14]. In particular, it has been shown that highly localized plasmons can exist in strip-like metal films [7-10], metal nano-rods [6], and quantum wires [11]. All of these structures can thus be used as sub-wavelength waveguides. In this case the localization of a guided plasmon can be far beyond what is allowed by the diffraction limit [6]. Highly localized surface plasmons were also shown to exist on the top of a trapezium metal wedge [12,13] and in a narrow gap between two rectangular pieces of metal [14].

Another direction in the development of sub-wavelength waveguides is related to nano-chains consisting of closely spaced identical metal nano-particles [1-5]. Each of these particles can sustain highly localized plasma oscillations that can be generated by an incident electromagnetic wave (Mie resonances) [3]. The guiding effect is realized when plasma oscillations of one particle are successively transported to other particles of the chain due to electric coupling. However, such nano-chain waveguides may be difficult to manufacture (due to strict tolerances on particle dimensions and separation). In addition, significant dissipation keeps the propagation distances under several hundreds of nanometers [1-3,5].

Very recently, a new type of localized plasmon (channel polaritons) guided by a curved metal surface in the form of a groove (e.g., of Gaussian shape) has been described theoretically [15]. The aim of this paper is to demonstrate that similar localized waves, called wedge channel polaritons (WCPs), can also exist near the tip of a triangular groove or dielectric wedge in a metallic medium. The main properties of WCPs in triangular grooves will be analyzed and discussed. Their existence conditions, dispersion and localization will be investigated.

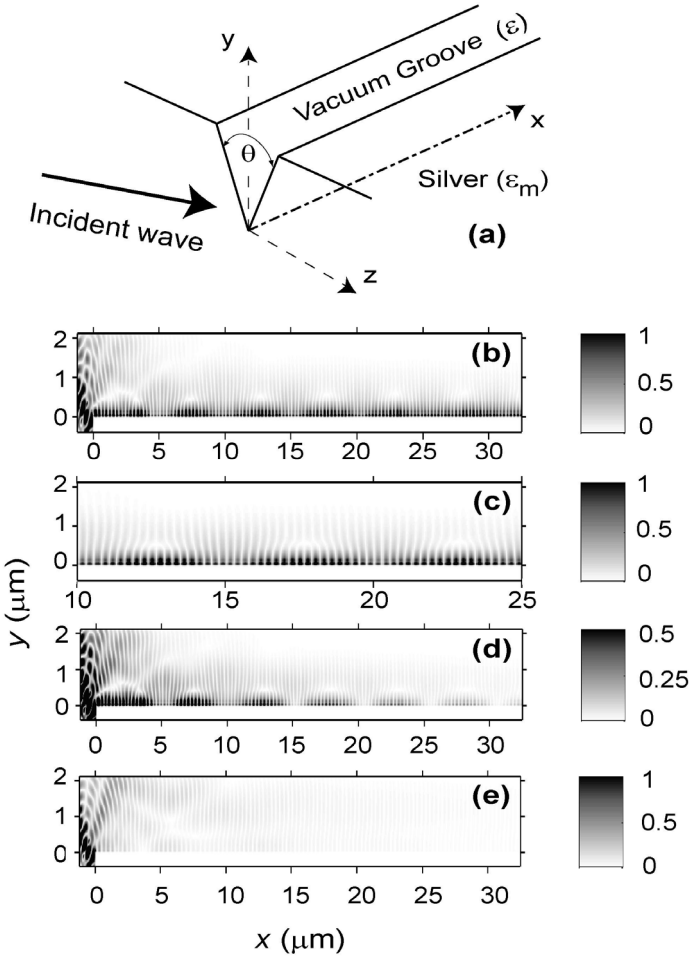

Fig. 1. (a) The structure with a triangular groove (dielectric wedge) in a metallic medium. (b) The distribution of the magnitude of the electric field in the vacuum groove ($\varepsilon = 1$) in silver with the free charge density $\rho \approx -7.684\times10^{9}$ C/m^{-3} [15] and damping frequency $f_d = 0$ (i.e., $\varepsilon_m = -16.22$ – no dissipation in the metal), resulting from the generation of WCPs by a bulk wave incident onto the end of the groove (at x = 0) at the angle of 45^{o}

with respect to the x-axis (Fig. 1a). The magnetic field in the incident wave is in the (x,y) plane, the groove angle $\theta = 30^o$, and λ(vacuum) = 0.6328 μm. (c) The magnified field structure from Fig. 1b for the interval 10 μm < x < 25 μm. (d) Same as in Fig. 1b, but with $f_d = 1.4332 \times 10^{13}$ Hz [15]: $\varepsilon_m = -16.22 + 0.52i$. (e) Same as in Fig. 1b, but for $\theta = 90^o$.

The analyzed structure is presented in Fig. 1a; ε_m and ε are permittivities of the metal and the material in the groove, respectively, θ is the angle of the groove. The depth of the groove is assumed to be infinite (sufficiently large to avoid edge effects). The metal with the groove occupies the region x > 0 (Fig. 1a), whereas at x < 0, we have a uniform dielectric medium with the permittivity ε that is the same as in the groove. To avoid the numerical instabilities associated with negative permittivity ε_m [16,17], the local Drude free-electron model has been incorporated into the FDTD algorithm [16,17]. As a result, ε_m is determined by the electron density in the metal. Artificial absorbing boundary conditions of the first-order Mur type have been used at the edges of the computational window [18].

WCPs are generated in the structure by the end-fire method, i.e. by assuming that a bulk wave of a wavelength λ in vacuum is incident onto the end of the groove at x = 0 (Fig. 1a). The specific structural parameters used for the numerical analysis are listed in the caption of Fig. 1. Figs. 1b-e present the typical distributions of the electric field in the middle of the groove as a function of x and y coordinates for two different angles $\theta = 30^o$ (Figs. 1b-d) and $\theta = 90^o$ (Fig. 1e). For Figs. 1b,c,e, dissipation in the metal was assumed to be zero, while the effect of dissipation is shown in Fig. 1d.

The main aspect that can be seen from Figs. 1b,c is the clear demonstration of the existence of a non-dissipating periodically changing electromagnetic field that is localized near the apex of the groove. This is the clear numerical evidence of existence of WCPs in the considered structure. Note that if the angle of the groove is $\geq 75^o$, then no localized wave has

been predicted for any polarization of the incident wave (Fig. 1e). This naturally suggests that WCPs can exist only at sufficiently small groove angles.

The periodic modulation of the field in the wave, clearly seen in Figs. 1b-d, is due to interference of different WCP modes. To analyze the mode structure of the generated signal (Figs. 1b,c), the field at the tip of the groove at $x > 0$ was expanded into the Fourier integral. The resultant Fourier amplitude as a function of wave vector is presented in Fig. 2a. The dominating wave number $q_1 \approx 1.195\times10^7$ m^{-1} corresponds to the fundamental WCP mode in the groove with the wavelength $\lambda_1 \approx 0.528$ μm.

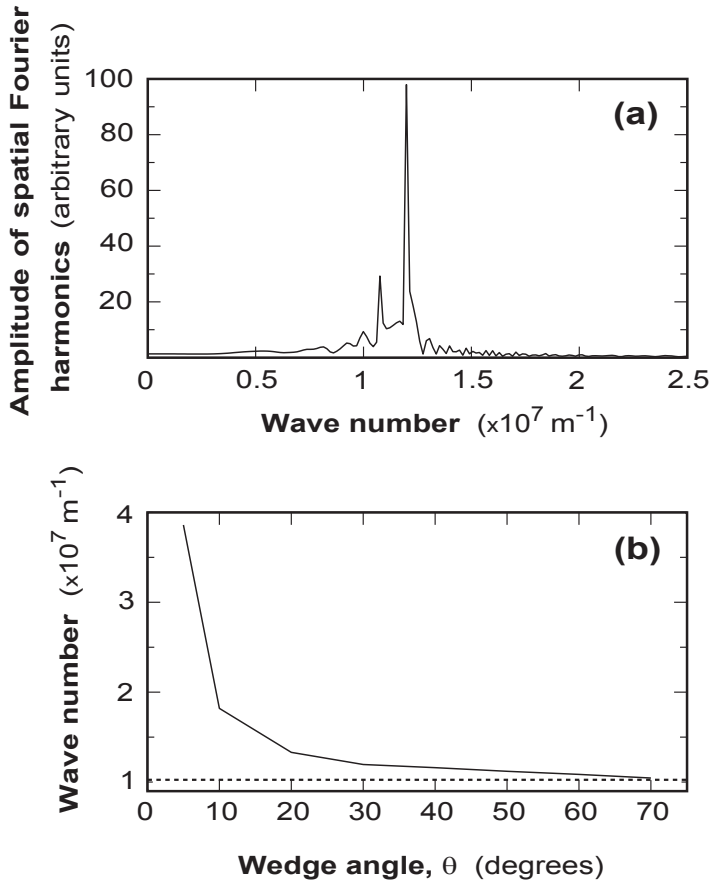

Fig. 2. (a) The dependence of the Fourier amplitude for the field at the tip of the groove (at $0 < x < 40$ μm in Fig. 1b) on wave vector. The two strong maxima correspond to two different WCP modes with $q_1 \approx 1.195\times10^7$ m^{-1} and $q_2 \approx 1.076\times10^7$ m^{-1}. (b) The dependence of the wave number q_1 of the fundamental WCP mode (the solid curve) on groove angle θ (10^o steps and an additional calculation at $\theta = 5^o$); the dotted line represents the wave number q_{sp} of the surface plasmon.

It can also be seen that there are two other distinct maxima at $q_2 \approx 1.076 \times 10^7$ m^{-1} and $q_3 \approx 1.0 \times 10^7$ m^{-1} on the left of the main maximum in Fig. 2a. The maximum at $q = q_2$ corresponds to the second WCP mode in the structure. Interference between the first (fundamental) and the second modes must give a pattern of beats with the period $\Lambda = 2\pi/(q_1 - q_2) \approx 6.43$ μm, which is in excellent agreement with the period of modulation of the field structure, that can clearly be seen in Figs. 1b,c.

One of the main existence conditions for a WCP is that its wave vector must be larger than the wave vector of surface plasmons on the sides of the groove. If this condition is not satisfied, then WCPs cannot exist, because they would leak into (generate) surface plasmons propagating away from the tip of the groove. It can be seen that the wave vector of the surface waves on a silver-vacuum interface is $q_{sp} \approx 1.025 \times 10^7$ m^{-1}, which is clearly less than the determined wave vectors of the two WCP modes.

In particular, it follows from here that the degree of localization of the second (or any higher) mode must be significantly less than that of the fundamental mode. This is related to the fact that increasing order of a mode results in decreasing its wave vector, and thus increasing penetration distance along the sides of the groove.

The third clear maximum in Fig. 2a at $q \approx q_{sp}$ can be explained by generation of surface plasmons on the sides of the groove and, possibly, by other unresolved higher WCP modes. The wave vectors of these modes (if they exist) are too close to the wave vector of surface plasmons, which makes their resolution fairly difficult (especially, taking into account poor efficiency of their generation).

It is reasonable to expect that the wave vector of the fundamental WCP mode must strongly depend on angle of the groove. For example, Fig. 1e suggests that generally there must be a cut-off angle for each of the WCP mode (the number of modes increases with decreasing angle of the groove). The solid curve in Fig. 2b presents the dependence of the wave

number q_1 of the fundamental WCP mode on angle of the groove. It can be seen that indeed, decreasing angle of the groove results in a rapid increase of the wave vector of the fundamental WCP mode. On the other hand, extrapolation of the curve to angles larger than 70^o leads to the conclusion that the upper cut-off angle for the considered structure is $\theta_c \approx 75^o$ (at which $q_1 = q_{sp}$). This is the reason for not seeing WCP in Fig. 1e.

The numerical analysis of the field structure in the groove and metal has suggested that for the fundamental mode at $\theta = 30^o$ the typical penetration depth of the field along the sides of the groove is ~ 170 nm from the tip, while across the groove (i.e., in along the z-axis) the localization of the wave is ~ 120 nm. Reduction of the groove angle results in increasing wave localization beyond the diffraction limit. This is directly related to increasing wave vector of WCP with decreasing groove angle (see Fig. 2b).

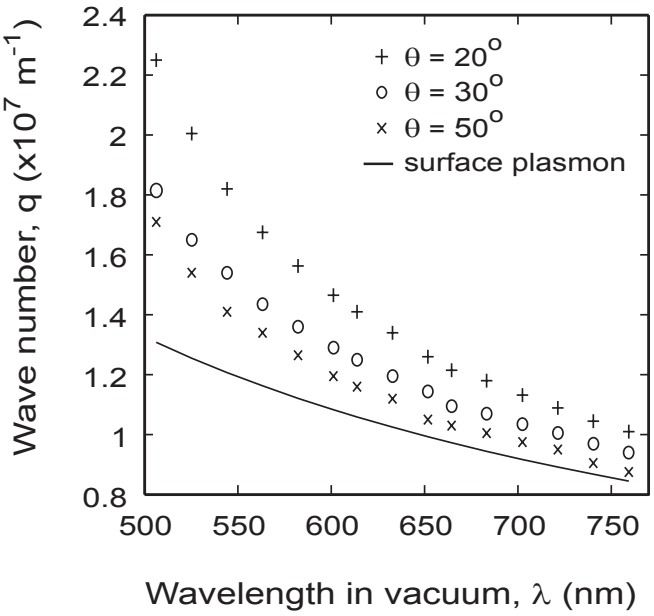

Fig. 3. The typical dispersion curves for WCPs in the silver-vacuum groove structure with three different angles θ. Solid curve: surface plasmons at an isolated smooth silver-vacuum interface.

The typical dispersion curves for WCPs in triangular grooves, obtained by means of the FDTD algorithm, are presented in Fig. 3. It can be seen that increasing λ (decreasing ω) results in decreasing wave vector of WCP for all groove angles. In this case, the localization of WCP is reduced due to the fact that its wave vector becomes closer to the wave vector of

surface plasmons at the sides of the groove (Fig. 3). On the contrary, decreasing λ (increasing ω) results in a rapid increase of the wave localization due to increasing its wave vector (especially for smaller angles θ – Fig. 3). Note that the dispersion of WPCs is solely due to dispersion of the dielectric permittivity in the metal ($-23.81 \le \varepsilon_m \le -10.02$ for Fig. 3). If it were not for the dispersion of $\varepsilon_m(\omega)$, WCPs would have been non-dispersive, because changing wavelength may only result in the proportional scaling of the field distribution in a triangular groove.

The numerical analysis has also suggested that typical dissipation of WCPs (Fig. 1d) is weaker than for other types of plasmon-based sub-wavelength waveguides with the same degree of lateral localization. However, this statement needs further confirmation by means of more consistent analysis of separate 1D modes rather than their interference pattern.

References

1. J. R. Krenn, Nature Mater. **2**, 210 (2003).
2. S. A. Maier, et al. Nature Mater. **2**, 229 (2003).
3. M. Quinten, A. Leitner, J. R. Krenn, F. R. Aussenegg, Opt. Lett. **23**, 1331 (1998).
4. B. Lamprecht, G. Schider, R. T. Lechner, H. Ditlbacher, J. R. Krenn, A. Leitner, F. R. Aussenegg, Phys. Rev. Lett. **84**, 4721 (2000).
5. S. A. Maier, P. G. Kik, H. A. Atwater, Appl. Phys. Lett. **81**, 1714 (2002).
6. J. Takahara, S. Yamagishi, H. Taki, A. Morimoto, T. Kobayashi, Opt. Lett. **22**, 475 (1997).
7. P. Berini, Optics Lett. **24**, 1011 (1999).
8. P. Berini, Phys. Rev. **B61**, 10484 (2000).
9. P. Berini, Phys Rev. B. **63**, 125417 (2001).
10. R. Charbonneau, P. Berini, E. Berolo, E. Lisicka-Shrzek, Opt. Lett. **25**, 844 (2000).

11. M. S. Kushwaha, Surf. Sci. Rep. **41**, 1 (2001).

12. T. Yatsui, M. Kougori, M. Ohtsu, Appl. Phys. Lett. **79**, 4583 (2001).

13. M. Ohtsu, K. Kobayashi, T. Kawazoe, S. Sangu, T. Yatsui, IEEE J. of Selected Topics in Quantum Electron. **8**, 839 (2002).

14. K. Tanaka, M. Tanaka, Appl. Phys. Lett. **82**, 1158 (2003).

15. I. V. Novikov, A. A. Maradudin, Phys. Rev. **B66**, 035403 (2002).

16. Christensen, D. Fowers, Biosens. Bioelectron. **11**, 677 (1996).

17. D. Fowers, Masters Thesis, University of Utah (1994).

18. G. Mur, IEEE Trans. Electromagnetic Compatibility **40**, 100 (1998).